frontiers in Earth Science

ORIGINAL RESEARCH
published: 20 August 2021
doi: 10.3389/feart.2021.740685

High Pressure Behaviors and a Novel High-Pressure Phase of Cuprous Oxide Cu_2O

Fei Qin[1]*, *Dongzhou Zhang*[2] *and Shan Qin*[3]

[1]School of Earth Sciences and Resources, China University of Geosciences (Beijing), Beijing, China, [2]School of Ocean and Earth Science and Technology, Hawai'i Institute of Geophysics and Planetology, University of Hawaii at Manoa, Honolulu, HI, United States, [3]School of Earth and Space Sciences, Peking University, Beijing, China

In the present study, we extensively explored the phase stabilities and elastic behaviors of Cu_2O with elevated pressures up to 29.3 GPa based on single-crystal X-ray diffraction measurements. The structural sequence of Cu_2O is different than previously determined. Specifically, we have established that Cu_2O under pressure, displays a cubic-tetragonal-monoclinic phase transition sequence, and a novel monoclinic high-pressure phase assigned to the *P*1*a*1 or *P*12/*a*1 space group was firstly observed. The monoclinic phase Cu_2O exhibits anisotropic compression with axial compressibility $\beta_b > \beta_c > \beta_a$ in a ratio of 1.00:1.64:1.45. The obtained isothermal bulk modulus of cubic and monoclinic phase Cu_2O are 125(2) and 41(6) GPa, respectively, and the K_{T0}' is fixed at 4. Our results provide new insights into the phase stability and elastic properties of copper oxides and chalcogenides at extreme conditions.

Keywords: Cu_2O, phase transitions, synchrotron single-crystal X-ray diffraction, copper compounds, high pressure

OPEN ACCESS

Edited by:
Lidong Dai,
Institute of Geochemistry (CAS), China

Reviewed by:
Fang Xu,
University College London, United Kingdom
Xiang Wu,
China University of Geosciences, China

***Correspondence:**
Fei Qin
fei.qin@cugb.edu.cn

Specialty section:
This article was submitted to Earth and Planetary Materials, a section of the journal Frontiers in Earth Science

Received: *13 July 2021*
Accepted: *11 August 2021*
Published: *20 August 2021*

Citation:
Qin F, Zhang D and Qin S (2021) High Pressure Behaviors and a Novel High-Pressure Phase of Cuprous Oxide Cu_2O. Front. Earth Sci. 9:740685. doi: 10.3389/feart.2021.740685

INTRODUCTION

The behaviors of transition metals and their oxides under high-temperature and high-pressure conditions have been studied extensively over a few decades, and knowledge about such material has important applications in physics, materials science, and engineering (Austin and Mott, 1970; Errandonea, 2006). Copper and its oxides are among the most investigated transition-metal materials. Cuprous oxide is a high-temperature semiconductor and one promising candidate materials for photo-electrochemical applications (Maksimov, 2000; Laskowski et al., 2003; Khanna et al., 2007). However, variations in physical properties and structural change of cuprous oxide Cu_2O at extreme conditions have not been fully investigated.

Cu_2O crystalizes in a simple cubic Bravais lattice with space group *Pn*-3*m* under normal thermodynamic conditions, while it has numerous structure forms at extreme conditions (Machon et al., 2003; Cortona and Mebarki, 2011; Feng et al., 2017). Most of previous studies have focused on the structural variations under high *P-T* conditions based on first-principles calculations. Cortona and Mebarki (2011) described the transition from cubic Cu_2O to the CdI_2-type structure (hexagonal, *R*-3*m*) at 10 GPa, while Feng et al. (2017) suggested two phase transitions, one at 5 GPa (*Pn*-3*m*→*R*-3*m*) and the other at 12 GPa (*R*-3*m*→*R*-3*m*1). However, this is hard to reconcile with some experimental results on the pressure-induced structural transformations of Cu_2O. A tetragonal phase was demonstrated by Machon et al. (2003) at pressures between 0.7 and 2.2 GPa using angle-dispersive powder X-ray diffraction (XRD), and another pseudocubic phase was detected at ~8.5 GPa. What is more, Sinitsyn et al. (2004) found a new hexagonal phase with lattice parameters of a = 5.86 Å and c = 18.78 Å at 21 GPa which was significantly different from those

reported earlier by Werner and Hochheimer (1982), who studied a hexagonal phase with $CdCl_2$-type structure with $a = 2.82$ Å and $c = 12.7$ Å measured at 18 GPa. Therefore, phase relations of Cu_2O at higher pressures are more sparse and show less mutual agreement. Further investigation is needed to study the exact high temperature and high pressures phases of Cu_2O.

There are limited studies on the behavior of cuprous oxides and copper chalcogenides under high pressure and high temperature conditions. In this present work, we report the phase transformations and elastic properties of Cu_2O up to ~30 GPa at room temperature, by using synchrotron-based single-crystal XRD with diamond anvil cell (DAC). We confirmed the tetragonal phase Cu_2O observed between 10.4 and 13.8 GPa, and a novel monoclinic phase at higher pressures is also reported. As is well-known, physical properties of materials can be modified by tailoring either chemical composition or microstructure. These results can improve our knowledge of how pressure affect their elastic and physical properties. In this report we also present the measured compressibilities and equations of states of these high pressure phases of Cu_2O.

MATERIALS AND METHODS

The cuprite measured in this study was originated from the Tonglushan Copper Miners in Daye, Hubei province. Single-crystal samples of natural, brick-red cuprite were selected as the starting material of our study. We screened several chips and polished them to ~10 μm in thickness. At ambient conditions, the Cu_2O was characterized in an empty diamond anvil cell (DAC) by single crystal X-ray diffraction, at the GSECARS beamline 13-BM-C of the Advanced Photon Source (APS), Argonne National Laboratory (Zhang et al., 2017). Diffraction collected at ambient conditions showed that the cuprite crystal had a *Pn*-3*m* space group with $a = 4.2733(7)$ Å, and the Cu_2O samples with a purity of 99.99% were used for the current study.

High-pressure compression measurements were performed, using short symmetric DACs fitted with Boehler-Almax diamond anvils with 300 μm flat culets and mounted into seats with 60° opening. Rhenium gaskets were preindented to ~40 μm thickness, and holes were drilled to ~170 μm diameter for the samples. On compression, the gasket thickness and sample chamber diameter both decrease to ~20 μm at the highest pressures reached. The polished Cu_2O sample was loaded together into the sample chamber along with Pt foil for pressure calibration (Fei et al., 2007). To achieve quasi-hydrostatic conditions and maintain similar pressure environments everywhere in the sample chamber, we loaded the cell with neon as the pressure-transmitting medium using the COMPRES/GSECARS gas-loading system (Rivers et al., 2008).

In situ high-pressure single-crystal X-ray diffraction experiments on Beamline 13-BM-C used a monochromatic X-ray beam with a wavelength of 0.4340 Å and focused to a 15×15 μm^2 spot. The experimental details were also described previously (Qin et al., 2017; Zhang et al., 2017). To obtain adequate number of diffraction peaks of samples and increase the coverage of the reciprocal space, we collected data at four different detector positions. The diffraction images were analyzed using the ATREX/RSV software package (Dera et al., 2013). Integrated diffraction data were analyzing using the DIOPTAS software (Prescher and Prakapenka, 2015), the high-pressure synchrotron XRD patterns were indexed by Dicvol06 (Louër and Boultif, 2007). Lattice parameters were calculated by the program UnitCell and the Le Bail refinement by GSAS (Holland and Redfern, 1997; Toby, 2001).

RESULTS

Tetragonal Phase

In situ X-ray diffraction patterns of Cu_2O were measured up to 29.3 GPa under hydrostatic pressure which presented in **Figure 1A**. At ambient conditions, all peaks can be indexed as the *Pn*-3*m* cubic structure (Hahn et al., 1983). When pressure increased to 16.1 GPa, an abrupt change in the integrated diffraction pattern was observed. As can be seen in the diffraction patterns in **Figure 1B**, reflections from the crystal show diffuse scattering and appear as short streaks at pressures above 16.1 GPa. Some diffraction peaks become fainter at higher angle, making it more difficult to determine the peak positions exactly (**Figure 1B**). We compared our integrated data of the high-pressure phase with previous studies but did not find any compatible structures (Werner and Hochheimer, 1982; Cortona and Mebarki, 2011; Feng et al., 2017).

A suspected phase transition from cubic to tetragonal between 0.7 and 2.2 GPa was reported previously (Machon et al., 2003), and our diffraction measurements confirmed this transition but at a different pressure (between 8.4 and 10.4 GPa, **Figure 2A**). We noticed that all the diffraction peaks deviated from a cubic lattice at pressures above 10.4 GPa, and can be well indexed as tetragonal lattice Cu_2O with space group $P4_2/nnm$. The high-pressure tetragonal phase Cu_2O at 10.4 GPa, was refined by Rietveld method in GSAS program shown in **Figure 2B**. The quality of the refinement is illustrated by the small *R*-factors and reduced X^2; $R_p = 0.18\%$, $R_{wp} = 0.25\%$, and $X^2 = 0.93$. As the tetragonal phase is the subgroup of the cubic phase (*Pn*-3*m*) and the two phases have very similar lattice parameters, i.e., for cubic phase, $a = 4.267$ Å and for tetragonal phase, $a = 4.193$, $a/c = 0.988$ (Hahn et al., 1983; Restori and Schwarzenbach, 1986; Machon et al., 2003). This tetragonal structure is also indicated by the asymmetry of the peaks centered at ~8.5°, 14.6°, 17° and 20°, resulting from the overlap of the (110)(011), (211)(112), (220)(202) and (131)(113) pairs of the tetragonal structure, respectively (**Figure 2A**). The tetragonal structure can be regarded as the distorted cubic structure under the uniaxial stress in the DAC.

Novel Monoclinic Phase

During the compression of Cu_2O, all the diffraction peaks move to larger 2θ values, as expected for pressure-induced bond shortening, and their intensities weaken gradually. When the pressure exceeds 16.1 GPa, some new peaks appeared (*d* spacings at ~2.83. 2.74, 2.42, 2.30, 2.03, 1.97, 1.76 Å and so on) and the *d*

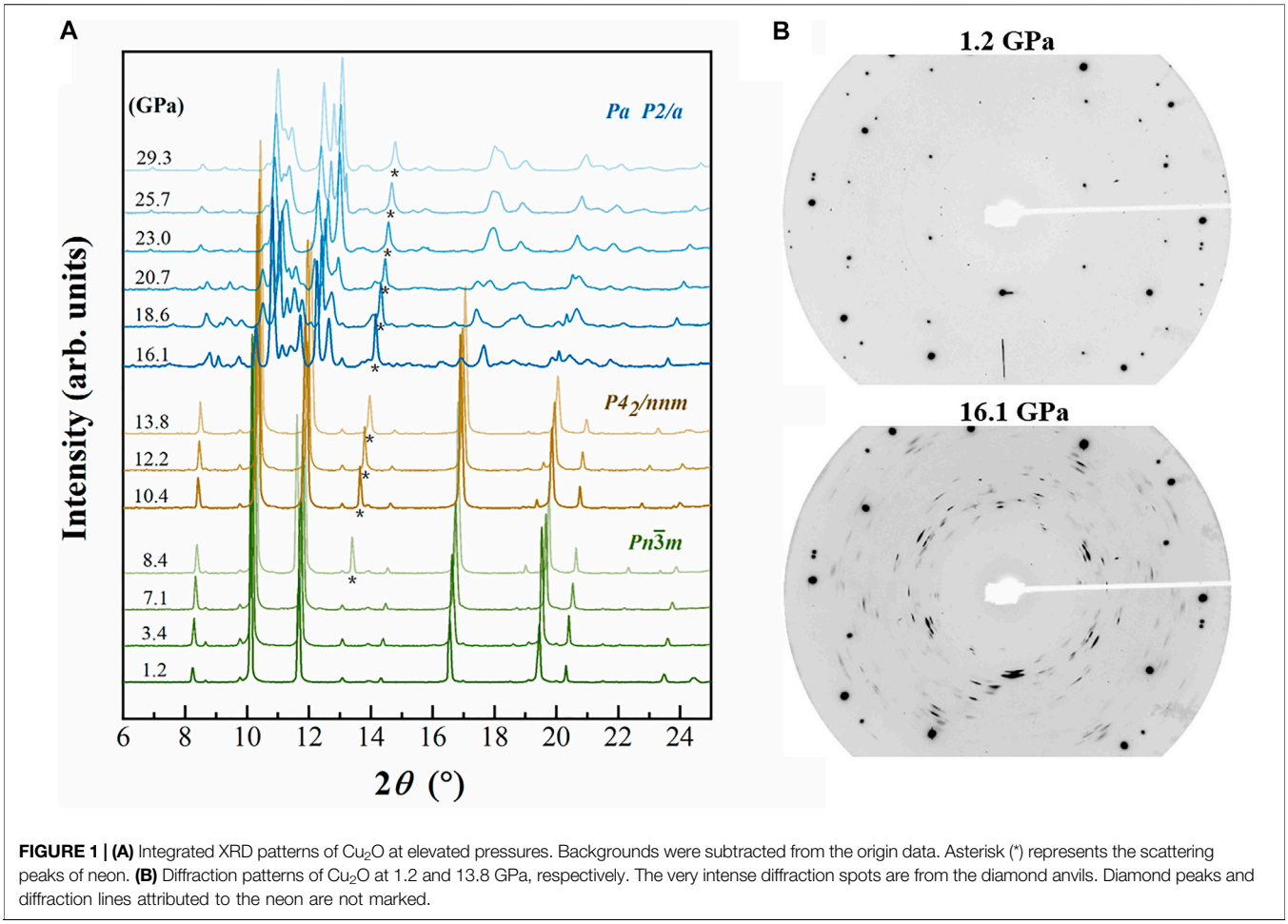

FIGURE 1 | (A) Integrated XRD patterns of Cu_2O at elevated pressures. Backgrounds were subtracted from the origin data. Asterisk (*) represents the scattering peaks of neon. **(B)** Diffraction patterns of Cu_2O at 1.2 and 13.8 GPa, respectively. The very intense diffraction spots are from the diamond anvils. Diamond peaks and diffraction lines attributed to the neon are not marked.

values of these peaks are totally different from those previous patterns, suggesting that the Cu_2O undergoes a reconstructive phase transition, and with further compression to the highest pressure, the structure can persist and no other transition was observed (**Figure 1A**). We have compared our patterns with some predicted hexagonal high-pressure phases of Cu_2O based on previous *ab initio* calculation and measurement results, but none of the predicted structures matches our measured diffraction pattern (Werner and Hochheimer, 1982; Cortona and Mebarki, 2011; Liu et al., 2014; Feng et al., 2017). In this case, the high quality data allow us to determine the crystal structure of the new high-pressure phase of Cu_2O. We chose several recognizable Debye rings, except for the neon rings, to index the crystal lattice using Dicvol06 software (Louër and Boultif, 2007). According to our results, the 16 chosen peaks of high-pressure phase Cu_2O, obtained at 16.1 GPa, can be successfully indexed as a monoclinic structure with the lattice parameters: a = 5.665(3) Å, b = 2.741(2) Å, c = 4.255(2) Å, β = 93.54(8)° and V = 65.94(2) Å^3 (**Table 1**).

Crystal lattice parameters, characteristic X-ray extinctions and diffracted intensities unambiguously documented that the crystal structure of the monoclinic phase Cu_2O belongs to the primitive lattice with no exception. $0k0$ manage the requirement of k = 2n + 1, and $h00$, $00l$ are also fulfilled the rules h = 2n and l = 2n. Consequently, space groups fulfilling these conditions are $P1a1$ (No. 7) and $P12/a1$ (No. 13) (Hahn et al., 1983). However, the quality of our diffraction pattern is not enough to differentiate the two space groups, as the space group Pa is a subgroup of $P2/a$, and both have very similar diffraction peak distributions.

Compressibility of Cu_2O

The P-V data of both Cu_2O phases were fitted using the third-order Birch-Murnaghan equation of state (BM3-EoS) with the data all equally weighted, since the errors in volume and pressure were similar for all measurements (Angle et al., 2014) (**Figure 3**). The refined lattice parameters of Cu_2O at various pressures are listed in **Table 2**. As the tetragonal structure could be regarded as the distorted cubic phase and the volumes of two phases only have marginal difference, thus we used cubic structure model to calculate the equation of state between 10.4 and 13.8 GPa to get higher accuracy. The resulting fitted parameters of volume, bulk modulus and its pressure derivative of cubic Cu_2O are as follows: V_0 = 78.05(3) Å^3, K_{T0} = 137(5) GPa and K_{T0}' = 1.8(7), respectively, which are 4.6% higher compared with the corresponding values from the experimental data from Werner and Hochheimer (1982), who reported 131 GPa when K' is 5.7. In

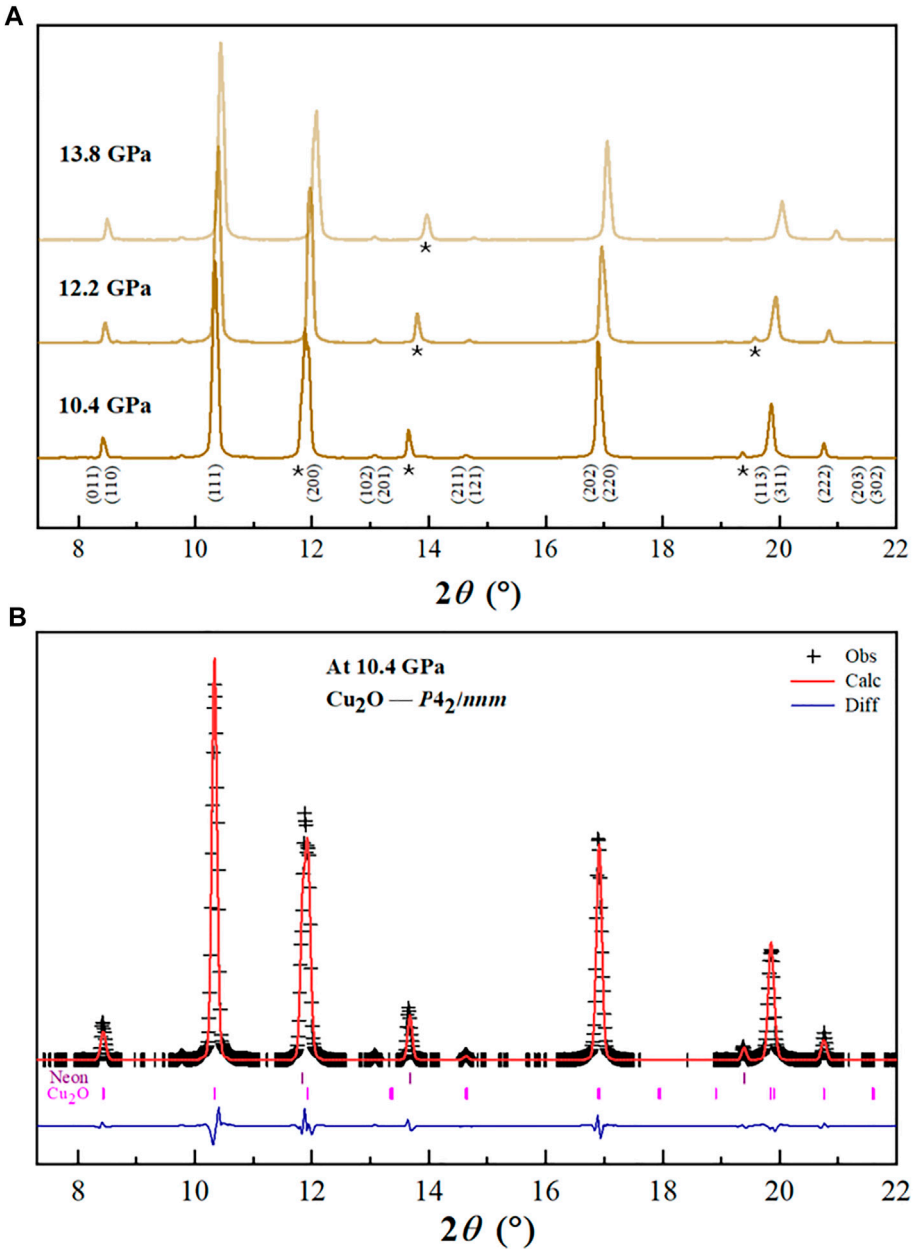

FIGURE 2 | (A) Selected XRD patterns of Cu_2O in the tetragonal phase. Asterisk (*) represents the scattering peaks of neon. **(B)** The Rietveld refinement of Cu_2O ($P4_2/nnm$). Observed and the calculated profiles are shown using black crosses and red solid line, respectively. The residual between them is shown by the blue line at the bottom. Bragg peak positions are indicated by the small ticks.

this present study, we also calculated the equation of state by fixing K_{T0}' at 4, resulting in K_{T0} = 125(2) GPa.

Here, we also firstly determined the elastic properties of the monoclinic phase Cu_2O using the EoSFit7c software (Angle et al., 2014). The measured lattice parameters are also provided in **Table 2**. The derived BM2-EoS (K_{T0}' = 4 implied) parameters yield the following bulk modulus K_{T0} = 41(6) GPa, and it is three times softer than the low-pressure phase. Axial compression behaviors are also presented in **Figure 4**. It is noteworthy that the *b*-axis possesses a larger axial compressibility compared with *a*- and *c*-axes, and therefore being the most compressible direction within the structure. The interaxial angle β has an increasing trend with compression.

DISCUSSION

The high-pressure behavior of cuprous oxide Cu_2O has attracted broad interests due to their various structures at different *P-T* conditions and its potential applications. Several previous studies

TABLE 1 | Calculated and Observed *d* spacings of a new monoclinic polymorph Cu_2O, as well as the normalized intensity I_{obs} for the *h k l* reflections.

h k l	d_{obs}	d_{cal}	d_{obs}-d_{cal}	$2\theta_{obs}$	$2\theta_{cal}$	$2\theta_{obs}$-$2\theta_{cal}$
200	2.8301	2.8274	0.0027	8.795	8.804	−0.008
010	2.741	2.7407	0.0003	9.082	9.082	−0.001
20-1	2.419	2.4234	−0.0044	10.293	10.275	0.019
011	2.3014	2.3028	−0.0016	10.823	10.815	0.008
002	2.124	2.1233	0.0007	11.728	11.732	−0.004
10-2	2.0315	2.0294	0.0021	12.267	12.277	0.01
210	1.971	1.9679	0.0031	12.642	12.662	−0.02
211	1.7613	1.7569	0.0044	14.157	14.189	−0.033
30-1	—	1.7636	−0.0026	—	14.135	0.021
21-2	1.4741	1.4753	−0.0012	16.932	16.917	0.015
003	1.4138	1.4155	−0.0017	17.656	17.637	0.019
212	—	1.4134	0.0007	—	17.664	−0.008
400	—	1.4137	−0.0003	—	17.66	−0.004
013	1.257	1.2577	−0.0007	19.882	19.871	0.011
11-3	1.2441	1.2422	−0.0019	20.092	20.121	−0.03
312	1.2243	1.2242	0.0001	20.424	20.42	0.004
41-1	—	1.2232	0.0009	—	20.438	−0.014
022	1.1511	1.1514	−0.0003	21.734	21.727	0.007
004	1.061	1.0616	−0.0006	23.603	23.589	0.014
023	0.984	0.9846	−0.0006	25.48	25.465	0.015

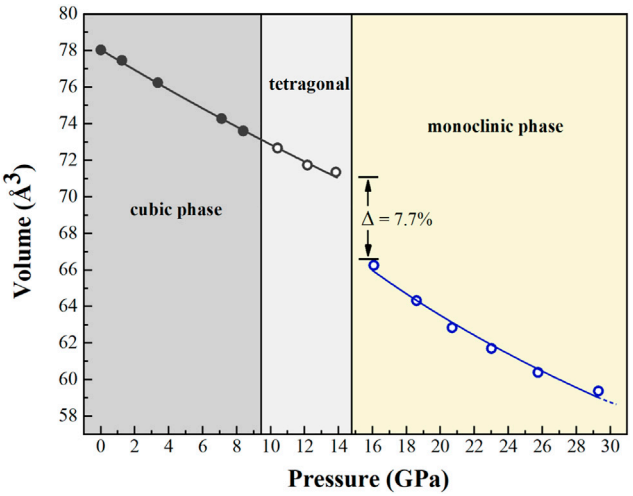

FIGURE 3 | The volume of Cu_2O as a function of pressure. A volume collapse of 7.7% at about 10.4–13.8 GPa, which is the location where the phase transition occurs between the tetragonal and monoclinic phases.

have been published which focus on the phase transitions and decompositions of Cu_2O and its thermodynamic properties as well (Machon et al., 2003; Sinitsyn et al., 2004; Cortona and Mebarki, 2011; Liu et al., 2014; Feng et al., 2017). However, these previous results were unclear about the high-pressure crystal structure of Cu_2O (tetragonal or hexagonal phase) and it is obvious that a large discrepancy of transformation pressure between the cubic and high-pressure phases existed between literatures. In this study, we re-confirmed the phase transition sequence from cubic-to-tetragonal phase occurred between 8.4 and 10.4 GPa using single-crystal XRD, which is significantly more higher than previously estimated (Machon et al., 2003). A new high-pressure phase of Cu_2O was also indexed using Dicvol06 software (Louër and Boultif, 2007). A volume collapse of ~7.7% in the region of 13.8–16.1 GPa was observed during the structural transformation from cubic to monoclinic phase (**Figure 3**). There is no indication of structural decomposition in this case. In addition, it is obvious that a considerable anisotropy in axial compressibility with $\beta_b > \beta_c > \beta_a$ and we found the ratio of zero-pressure axial compressibility is 1.00:1.64:1.45 according to our data. Thus, it can be concluded that the largest anisotropy in compressibility is along the *b* axis, which behaves about twice as compressible than the *a*-axis in the structure (**Figure 4**). Further investigation should be done to investigate the exact high temperature phases of Cu_2O.

In some recent studies, several members of copper chalcogenides, such as Cu_2S and Cu_2Se have been theoretically proposed and experimentally exhibited as the thermoelastic materials (Danilkin et al., 2011; Santamaria-Perez et al., 2014; Zhang et al., 2018; Zimmer et al., 2018; Xue et al., 2019). The high-pressure phase Cu_2O, Cu_2Se and Cu_2S may adopt the same monoclinic structure at different pressure conditions, which indicates that these copper compounds may have a similar crystal chemistry configuration (Santamaria-Perez et al., 2014; Zhang et al., 2018). The structural complexity of Cu_2S have been studied previously, in which two phase transitions occurred at 3.2 and 7.4 GPa from the *P*21/*c* phase to two different monoclinic structures (Santamaria-Perez et al., 2014). Pressure-induced structural transition sequence is also identified in Cu_2Se. The initial low-pressure phase (*C*2/*c*) transformed to phase II and semimetallic phase III at 3.2 GPa, and then followed by a reconstructive transformation to bulk metallic phase IV (*Pca*21) at 7.4 GPa. These mentioned phases could be confidently associated with the electronic state transitions (Zhang et al., 2018; Chuliá-Jordan et al., 2020). As for the copper sulfide, three phase-transitions occurred at 3.2, 7.4 and 26 GPa, respectively, and there is a significant difference of the reported values of bulk modulus, ranging from 72 to 113 GPa (Santamaria-Perez et al., 2014). The determination of the phase stability of such stoichiometric copper oxides under compression will give more insight into possible systematic trends in group copper chalcogenides, and provide a direct comparison with such thermoelastic materials at extreme conditions where their phase behaviors could converge.

CONCLUSION

The high-pressure behaviors of cuprous oxide Cu_2O have been studied by synchrotron-based single-crystal XRD at pressures up to ~30 GPa at 300 K conditions. The initial low-pressure cubic phase transforms to distorted $P4_2/nnm$ phase between 10.4 and 13.8 GPa, and the tetragonal structure persisted at pressure up to ~16 GPa. A new high-pressure phase of Cu_2O (monoclinic phase,

TABLE 2 | Lattice parameters of Cu_2O (cubic, tetragonal and monoclinic phases) at various pressures.

Pressure (GPa)	a (Å)	b (Å)	c (Å)	B	V (Å^3)	Symmetry
0.00001	4.2733(7)	—	—	—	78.04(2)	Cubic
1.2[a]	4.2630(6)	—	—	—	77.47(9)	—
3.4	4.2405(6)	—	—	—	76.25(9)	—
7.1	4.2036(6)	—	—	—	74.28(9)	—
8.4	4.1909(5)	—	—	—	73.61(7)	—
10.4	4.174(2)	4.174(2)	4.171(3)	—	72.67(7)	Tetragonal
12.2	4.157(2)	4.157(2)	4.152(3)	—	71.75(7)	—
13.8	4.147(3)	4.147(3)	4.149(4)	—	71.36(10)	—
16.1	5.696(2)	2.737(1)	4.2568(8)	93.17(3)	66.26(2)	Monoclinic
18.6	5.639(3)	2.704(1)	4.2237(8)	92.98(3)	64.33(2)	—
20.7	5.615(2)	2.675(1)	4.1913(7)	93.08(3)	62.85(2)	—
23.0	5.577(2)	2.661(1)	4.1645(7)	93.24(3)	61.71(2)	—
25.7	5.533(2)	2.647(1)	4.1307(7)	93.47(3)	60.40(2)	—
29.3	5.520(2)	2.630(1)	4.0997(7)	93.60(3)	59.38(2)	—

[a]*Nominal uncertainty in pressure in ±0.1 GPa.*

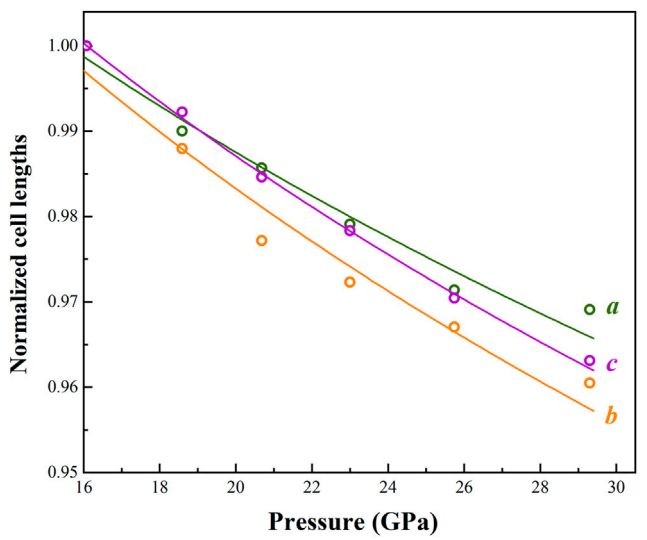

FIGURE 4 | Pressure dependence of normalized cell lengths (a, b and c) of monoclinic phase Cu_2O. EoS fits in the current study are shown by solid curves.

*P*1a or *P*12/*a*1) was obtained at 16.1 GPa at room temperature and the high-pressure elastic properties was firstly measured in this study. It is expected that the three times more compressible high-pressure phase Cu_2O may process some advantages properties than previously thought. The findings contribute to broadening our knowledge of the crystal chemistry of cuprite at high-pressure conditions, thus giving a better understand of thermoelastic materials in the copper chalcogenide system.

DATA AVAILABILITY STATEMENT

The original contributions presented in the study are included in the article/Supplementary Material, further inquiries can be directed to the corresponding author.

AUTHOR CONTRIBUTIONS

FQ and DZ carried out the experiments. FQ, DZ, and SQ performed the data analysis and interpretation. FQ wrote the manuscript. All authors contributed to the discussion of the results and revisions of the manuscript.

FUNDING

This research was supported by the Fundamental Research Funds for the Central Universities (grant no. 590421013) and the National Natural Science Foundation of China (grant no. 42072047). Work performed at GSECARS (Sector 13) of the Advanced photon Source (APS) is supported by the NSF EAR-1634415 and the Department of Energy (DOE) DE-FG02- 94ER1446. The APS at Argonne National Laboratory is supported by the DOE, Office of Science, under Contract No.DE-AC02-06CH11357. Experiments at Sector 13-BM-C of the APS used the PX2 facility, supported by GSECARS and COMPRES under NSF Cooperative Agreement EAR-1661511.

ACKNOWLEDGMENTS

We also thank S.Tkachev for gas loading the diamond cells.

REFERENCES

Angel, R. J., Alvaro, M., and Gonzalez-Platas, J. (2014). EosFit7c and a Fortran Module (Library) for Equation of State Calculations. *Z. Kristallogr.* 229, 405–419. doi:10.1515/zkri-2013-1711

Austin, I. G., and Mott, N. F. (1970). Metallic and Nonmetallic Behavior in Transition Metal Oxides. *Science* 168, 71–77. doi:10.1126/science.168.3927.71

Chuliá-Jordan, R., Santamaría-Pérez, D., Pereira, A. L. J., García-Domene, B., Vilaplana, R., Sans, J. A., et al. (2020). Structural and Vibrational Behavior of Cubic Cu1.80(3)Se Cuprous Selenide, Berzelianite, under Compression. *J. Alloys Compd.* 830, 154646. doi:10.1016/j.jallcom.2020.154646

Cortona, P., and Mebarki, M. (2011). Cu2O Behavior under Pressure: Anab Initiostudy. *J. Phys. Condens. Matter* 23, 045502. doi:10.1088/0953-8984/23/4/045502

Danilkin, S. A., Avdeev, M., Sakuma, T., Macquart, R., and Ling, C. D. (2011). Neutron Diffraction Study of Diffuse Scattering in Cu2−δSe Superionic Compounds. *J. Alloys Compd.* 509, 5460–5465. doi:10.1016/j.jallcom.2011.02.101

Dera, P., Zhuravlev, K., Prakapenka, V., Rivers, M. L., Finkelstein, G. J., Grubor-Urosevic, O., et al. (2013). High Pressure Single-crystal Micro X-ray Diffraction Analysis with GSE_ADA/RSV Software. *High Press. Res.* 33, 466–484. doi:10.1080/08957959.2013.806504

Errandonea, D. (2006). Phase Behavior of Metals at Very High P-T Conditions: A Review of Recent Experimental Studies. *J. Phys. Chem. Sol.* 67, 2017–2026. doi:10.1016/j.jpcs.2006.05.031

Fei, Y., Ricolleau, A., Frank, M., Mibe, K., Shen, G., and Prakapenka, V. (2007). Toward an Internally Consistent Pressure Scale. *Proc. Natl. Acad. Sci.* 104, 9182–9186. doi:10.1073/pnas.0609013104

Feng, W., Ren, W., Yu, J., Zhang, L., Shi, Y., and Tian, F. (2017). High-pressure Phase Transitions of Cu 2 O. *Solid State. Sci.* 74, 70–73. doi:10.1016/j.solidstatesciences.2017.09.011

Hahn, T., Shmueli, U., and Arthur, J. C. W. (1983). *International Tables for Crystallography. Vol. 1*. Dordrecht: Reidel.

Holland, T. J. B., and Redfern, S. A. T. (1997). UNITCELL: a Nonlinear Least-Squares Program for Cell-Parameter Refinement and Implementing Regression and Deletion Diagnostics. *J. Appl. Cryst.* 30, 84. doi:10.1107/S0021889896011673

Khanna, P. K., Gaikwad, S., Adhyapak, P. V., Singh, N., and Marimuthu, R. (2007). Synthesis and Characterization of Copper Nanoparticles. *Mater. Lett.* 61, 4711–4714. doi:10.1016/j.matlet.2007.03.014

Laskowski, R., Blaha, P., and Schwarz, K. (2003). Charge Distribution and Chemical Bonding inCu2O. *Phys. Rev. B* 67, 075102. doi:10.1103/PhysRevB.67.075102

Liu, K., Duan, Y.-F., Lv, D., Wu, H.-B., Qin, L.-X., Shi, L.-W., et al. (2014). Pressure-Induced Cubic-To-Hexagonal Phase Transition in Cu 2 O. *Chin. Phys. Lett.* 31, 117701. doi:10.1088/0256-307X/31/11/117701

Louër, D., and Boultif, A. (2007). Powder Pattern Indexing and the Dichotomy Algorithm. *Z. Kristallogr. Suppl.* 2007, 191–196. doi:10.1524/zksu.2007.2007.suppl_26.191

Machon, D., Sinitsyn, V. V., Dmitriev, V. P., Bdikin, I. K., Dubrovinsky, L. S., Kuleshov, I. V., et al. (2003). Structural Transitions in Cu2O at Pressures up to 11 GPa. *J. Phys. Condens. Matter* 15, 7227–7235. doi:10.1088/0953-8984/15/43/007

Maksimov, E. G. (2000). High-temperature Superconductivity: the Current State. *Phys.-Usp.* 43, 965–990. doi:10.1070/PU2000v043n10ABEH000770

Prescher, C., and Prakapenka, V. B. (2015). DIOPTAS: a Program for Reduction of Two-Dimensional X-ray Diffraction Data and Data Exploration. *High Press. Res.* 35, 223–230. doi:10.1080/08957959.2015.1059835

Qin, F., Wu, X., Zhang, D., Qin, S., and Jacobsen, S. D. (2017). Thermal Equation of State of Natural Ti-Bearing Clinohumite. *J. Geophys. Res. Solid Earth* 122, 8943–8951. doi:10.1002/2017JB014827

Restori, R., and Schwarzenbach, D. (1986). Charge Density in Cuprite, Cu2O. *Acta Crystallogr. Sect B* 42, 201–208. doi:10.1107/S0108768186098336

Rivers, M., Prakapenka, V., Kubo, A., Pullins, C., Holl, C., and Jacobsen, S. (2008). The COMPRES/GSECARS Gas-Loading System for diamond Anvil Cells at the Advanced Photon Source. *Ghpr* 28, 273–292. doi:10.1080/08957950802333593

Santamaria-Perez, D., Garbarino, G., Chulia-Jordan, R., Dobrowolski, M. A., Mühle, C., and Jansen, M. (2014). Pressure-induced Phase Transformations in mineral Chalcocite, Cu2S, under Hydrostatic Conditions. *J. Alloys Compd.* 610, 645–650. doi:10.1016/j.jallcom.2014.04.176

Sinitsyn, V. V., Dmitriev, V. P., Bdikin, I. K., Machon, D., Dubrovinsky, L., Ponyatovsky, E. G., et al. (2004). Amorphization of Cuprite, Cu2O, Due to Chemical Decomposition under High Pressure. *Jetp Lett.* 80, 704–706. doi:10.1134/1.1862798

Toby, B. H. (2001). EXPGUI, a Graphical User Interface forGSAS. *J. Appl. Cryst.* 34, 210–213. doi:10.1107/S0021889801002242

Werner, A., and Hochheimer, H. D. (1982). High-pressure X-ray Study ofCu2O andAg2O. *Phys. Rev. B* 25, 5929–5934. doi:10.1103/PhysRevB.25.5929

Xue, L., Zhang, Z., Shen, W., Ma, H., Zhang, Y., Fang, C., et al. (2019). Thermoelectric Performance of Cu2Se Bulk Materials by High-Temperature and High-Pressure Synthesis. *J. Materiomics* 5, 103–110. doi:10.1016/j.jmat.2018.12.002

Zhang, D., Dera, P. K., Eng, P. J., Stubbs, J. E., Zhang, J. S., Prakapenka, V. B., et al. (2017). High Pressure Single crystal Diffraction at PX2̌. *JoVE* 119, e54660. doi:10.3791/54660

Zhang, Y., Shao, X., Zheng, Y., Yan, L., Zhu, P., Li, Y., et al. (2018). Pressure-induced Structural Transitions and Electronic Topological Transition of Cu2Se. *J. Alloys Compd.* 732, 280–285. doi:10.1016/j.jallcom.2017.10.201

Zimmer, D., Ruiz-Fuertes, J., Morgenroth, W., Friedrich, A., Bayarjargal, L., Haussühl, E., et al. (2018). Pressure-induced Changes of the Structure and Properties of Monoclinic α -chalcocite Cu2S. *Phys. Rev. B* 97, 134111. doi:10.1103/PhysRevB.97.134111

Conflict of Interest: The authors declare that the research was conducted in the absence of any commercial or financial relationships that could be construed as a potential conflict of interest.

Publisher's Note: All claims expressed in this article are solely those of the authors and do not necessarily represent those of their affiliated organizations, or those of the publisher, the editors and the reviewers. Any product that may be evaluated in this article, or claim that may be made by its manufacturer, is not guaranteed or endorsed by the publisher.